# Cluster discrimination in electrostatic heteroaggregation processes

J. M. López-López, A. Schmitt, J. Callejas-Fernández, and R. Hidalgo-Álvarez*
*Biocolloid and Fluid Physics Group, Department of Applied Physics, University of Granada, Campus de Fuentenueva, E-18071 Granada, Spain*

(Received 2 August 2003; published 29 January 2004)

Electrostatic heteroaggregation processes arising in 1:1 mixtures of oppositely charged microspheres at low and very low electrolyte concentrations were investigated by means of single-cluster light scattering. Cluster discrimination, i.e., the fact that clusters differing by only one constituent particle behave quite differently, was found for monomers and dimers. This effect was recently predicted by Brownian dynamic simulations but, to the best of our knowledge, not yet confirmed by experiments. The experimental data were confronted with the simulations and a good qualitative and quantitative agreement was obtained. The origin of the cluster discrimination phenomenon could be related to the range of the attractive electrostatic interactions.

DOI: 10.1103/PhysRevE.69.011404 PACS number(s): 82.70.Dd, 61.43.Hv, 05.40.−a

## I. INTRODUCTION

Aggregation of colloidal systems formed by oppositely charged particles, usually referred to as electrostatic heteroaggregation, is important in many technological processes, including mineral flotation [1], cell recovery [2], stability of emulsions [3], and synthesis of engineering ceramics [4]. Heteroaggregation, however, is not as extensively studied as homoaggregation, i.e., the aggregation of monocomponent colloidal dispersions. This may be mainly due to the relatively complex interactions between dissimilar particles that the classical Derjaguin-Landau-Verwey-Overbeek theory [5,6] cannot account for [7,8]. While the overlapping of the electrical double layers surrounding two like particles is always unfavorable, this is not necessarily the case when unlike particles approach each other. At low electrolyte concentrations, attractive interactions between oppositely charged particles can even increase the aggregation rate to values above the diffusion limit [9,10].

Recently, Puertas *et al.* [11] reported an interesting effect arising at very low electrolyte concentration in simulated 1:1 mixtures of equally sized particles with opposite electric surface charge. They found that the cluster concentration profiles exhibit a noncontinuous behavior at relatively long aggregation times. In other words, clusters differing by only one constituent particle behave quite differently. They named this effect *cluster discrimination*.

To the best of our knowledge, cluster discrimination has not yet been confirmed by experiments although several experimental studies about electrostatic heteroaggregation at low electrolyte concentration are reported in literature [3,10,12–18]. The reason is that in most of these studies, multiparticle techniques such as static and dynamic light scattering were employed to monitor aggregation. These techniques, however, provide only average information on the cluster-size distribution (CSD) and so, cannot resolve clusters that differ by one constituent particle. Evidently, single-cluster detection techniques are the techniques of choice. Although Stoll and Pefferkorn [12] employed a Coulter counter as such a technique, they also did not detect cluster discrimination. A possible explanation for this is that they used relatively large particles ($\simeq 1\ \mu$m) and fixed the $p$H of the aqueous medium at 4.2. This leads to a $\kappa a$ value of approximately 15 which is by far larger than the limit where cluster discrimination is predicted by Puertas *et al.* in their Brownian dynamics simulations ($\kappa a \lesssim 5$). Here, $\kappa a$ is the widely used product of the inverse of the Debye screening length, $\kappa$, and the particle radius $a$.

The aim of this work is to study experimental electrostatic heteroaggregation processes under conditions where cluster discrimination is expected to occur and to contrast the obtained results with the predictions made by Puertas *et al.* As suggested by James *et al.* [19], the best way for a quantitative test of the theory of heteroaggregation is to use amphoteric latexes and to study their interactions with an ionic latex of the same material. In these systems, the range and intensity of the electrostatic interaction can be tuned varying the electrolyte concentration. Moreover, the ratio between the surface charges of both particles can be adjusted fixing the medium $p$H. For this work, we employed a system of such characteristics. We chose, however, smaller particles than Stoll and Pefferkorn and left the $p$H free in order to achieve lower $\kappa a$ values. We studied the heteroaggregation processes arising in 1:1 mixtures at low and very low electrolyte concentrations and used single-cluster light scattering (SCLS) as single-cluster detection technique for monitoring the time evolution of the cluster-size distribution.

This paper is organized as follows: the experimental system and techniques are described in Sec. II. Section III is divided into two subsections: the SCLS measurements are presented in Sec. III A and compared with simulations of Puertas *et al.* in Sec. III B. Finally, the conclusions are summarized in Sec. IV.

## II. MATERIALS AND METHODS

The water used in this study was obtained using Millipore equipment (Milli-Q Academic System, Millipore Corporation, Massachusetts) which provides water with a conductivity smaller than 0.055 $\mu$S cm$^{-1}$. The temperature of all re-

*Electronic address: rhidalgo@ugr.es

 

TABLE I. Particle diameter ($2a$), polydispersity index (PDI), and electrophoretic mobility ($\mu_e$) at free $p$H and 2m$M$ KBr for both experimental systems.

| Particles | $2a$ (nm) [a] | PDI [a] | $\mu_e(10^{-8}\ m^2\ V^{-1}\ s^{-1})$ [b] |
|---|---|---|---|
| Sulfate | $524\pm19$ | 1.005 | $-(4.82\pm0.14)$ |
| Amidine | $525\pm14$ | 1.002 | $+(4.72\pm0.05)$ |

[a]Transmission electron microscopy (TEM).
[b]Zeta-Sizer IV, Malvern Instruments UK.

actants was stabilized at $(20\pm1)$ °C several hours before aggregation was started.

Following the suggestions of James *et al.* [19], two polystyrene latexes were used as model colloidal dispersions. The amphoteric amidine latex was supplied by Interfacial Dynamics Corporation (IDC, Portland, Oregon). The anionic sulfate latex was synthesized in our laboratories according to the recipe described by Goodwin *et al.* [20]. Already for homoaggregation experiments, highly monodisperse microspheres are required in order to distinguish clusters of different size with SCLS. Hence, much care was taken that both systems used for the heteroaggregation experiments were as similar in size as possible. Therefore, we checked the particle size by means of transmission electron microscopy and found that the particle size distributions of both selected systems match almost completely, i.e., both distributions peak at the same particle size although the amidine latex particles are slightly more monodisperse (see Table I).

$p$H buffering was avoided in order to keep the ionic concentration as low as possible. At free $p$H, the amidine latex particles bare positive surface charge while the sulfate latex particles remain negatively charged. This was checked by electrophoretic mobility measurements (Zeta Sizer IV, Malvern Instruments, UK) using 2.0m$M$ KBr as reference electrolyte concentration. The obtained results are summarized in Table I. As can be seen, the absolute values of the electrophoretic mobility, $|\mu_e|$, of both systems are very similar. This means that also other phenomena related to the particle surface charge, such as electrostatic interactions, are expected to be of the same order.

Since no buffers could be used for the aggregation experiments, the $p$H of the particle suspensions could vary slightly when mixing both particle dispersions. In order to check that these variations do not alter the electrophoretic mobility, we measured $\mu_e$ of both systems as a function of the $p$H using buffers of low ionic strength (2m$M$). The obtained results (see Fig. 1) confirm that the electrophoretic mobility of both, the amidine and sulfate latex particles, remains approximately constant in the free $p$H region around 5.5.

The single-cluster light scattering (SCLS) instrument used in this work allows us to obtain the cluster-size distribution for small aggregates without any assumptions about the cluster structure. In our SCLS device, the colloidal dispersion is injected into a fast double-distilled and 0.22-$\mu$m-filtered water flow by means of a computer-controlled peristaltic pump (Minipuls 312, Gilson, France). The clusters, separated by this hydrodynamic focusing, are then forced to flow across a focused laser beam. The light pulses that they scatter are

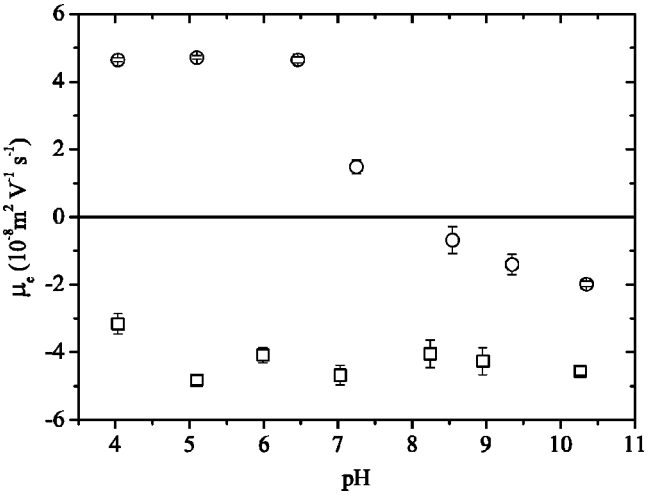


FIG. 1. Electrophoretic mobility of the amidine (○) and sulfate (□) latex particles vs the $p$H of the suspension.

detected at small scattering angle and counted and classified according to their intensity. Since the scattered light intensity at low angle is monotonically related to the cluster volume, the CSD is obtained. Our instrument is capable of distinguishing aggregates composed of up to eight particles $[c_n(t), n\leqslant 8]$. Furthermore, the total number of scattered light pulses, i.e., the total number of clusters ($\Sigma_n c_n$), is also available. A more detailed description of this technique can be found elsewhere [21,22].

Prior to the aggregation experiments, the amidine and sulfate particle dispersions were prepared at a particle concentration of $2\times10^8$ cm$^{-3}$ and sonicated for 10 min in an ultrasonic bath (Ultrasons, Selecta, 150 W) in order to approach monomeric initial conditions. Heteroaggregation was started by mixing 20 ml of KBr electrolyte solution and 10 ml of each sample by means of Y-shaped mixing devices. The total particle concentration of the resulting mixture was always $c_0=10^8$ cm$^{-3}$. This particle concentration is low enough to ensure single particle detection during the whole measuring process. The final KBr concentrations were 0m$M$, 0.01m$M$, 0.1m$M$, 1.0m$M$, and 10m$M$. Here, 0m$M$ means that pure water was added instead of electrolyte solution. For comparing purposes, also one aggregation experiment at high electrolyte concentration (1.0$M$) was performed. Precipitation was not observed during the duration of the experiments.

## III. RESULTS AND DISCUSSION

### A. Experimental cluster-size distributions

Pure electrostatic heteroaggregation arising in 1:1 mixtures of positively and negatively charged particles was investigated at low and very low ionic concentrations. Evidently, the smallest possible ionic concentration is achieved when no electrolyte is added. In this case, the ionic concentration is mainly due to the medium $p$H and was estimated to be smaller than $3\mu M$. Starting from there, the ionic concentration was increased up to 10m$M$ using KBr as indifferent 1:1 electrolyte. Since both, the amidine and sulfate latex particles, remain kinetically stable for electrolyte concentrations

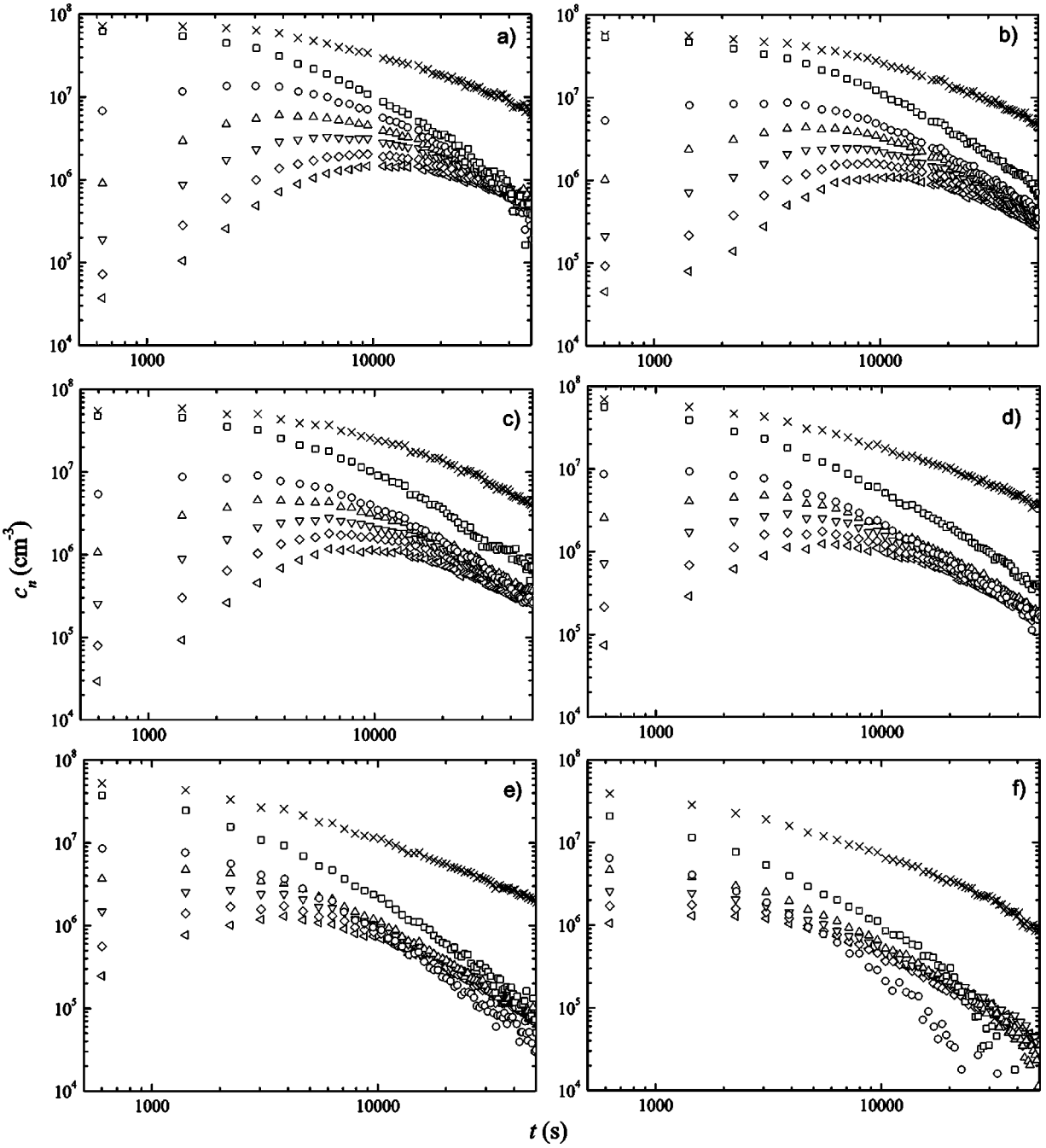


FIG. 2. Time evolution of the cluster-size distributions for different KBr concentrations: (a) 1.0*M*, (b) 10m*M*, (c) 1.0m*M*, (d) 0.1m*M*, (e) 0.01m*M*, and (f) no added electrolyte. In each plot, the monomer (□), dimer (○), trimer (△), tetramer (▽), pentamer (◇), hexamer (◁) concentrations and the total concentration of aggregates (×) are shown.

smaller than 10m*M* KBr, no significant contribution from homoaggregation is expected for all these heteroaggregation experiments.

An additional experiment was performed at 1.0*M* KBr, where both, the amidine and the sulfate latex particles, are completely unstable and aggregate in the diffusion-limited colloid aggregation regime (DLCA) [23]. This means that the electrical double layers are confined to the particle surface and only short range attractive interactions are acting. Consequently, the attractive electrostatic interaction between unlike particles is also screened and the mixed system behaves like a monocomponent one in the DLCA regime [24]. Although in this case homoaggregation and heteroaggregation will take place simultaneously, it is included here for comparing purposes.

Figure 2 shows the time evolution of the cluster-size distributions for clusters formed by up to six monomeric particles (hexamers) and the total cluster concentration. It should be mentioned that a *n*-mer curve in these plots comprises all possible types of clusters formed by *n* monomers. For example, the trimer concentration curve includes all possible types of trimers such as positive-negative-positive and

negative-positive-negative trimers. This is due to the fact that equally sized monomeric particles have been used and so, all clusters formed by the same number of constituent particles scatter the same amount of light.

All studied aggregation processes shown in Fig. 2 exhibit some common features.

(i) Evidently, they start from monomeric initial conditions.

(ii) The monomer concentration decreases monotonically since monomers cannot be created under the given experimental conditions.

(iii) Larger aggregates have to be formed before they can react with other clusters and so, the corresponding curves exhibit a maximum.

(iv) At long aggregation times, all curves show a decreasing tendency which means that no dynamic equilibrium is reached. Consequently, the underlying aggregation mechanisms seem to be of irreversible nature.

(v) Since no precipitation was observed during the experiments, the always decreasing behavior of the total cluster concentration curves implies that the average cluster size keeps growing. This means that larger aggregates must be present although their size could not be resolved by the employed detection technique.

Before we comment on the aggregation experiments at low and very low electrolyte concentration, we would like to discuss the experiment at 1.0*M* KBr. As mentioned before, the 1:1 mixture of positively and negatively charged particles at high electrolyte concentration is expected to aggregate in the DLCA regime. In order to prove this hypothesis, we performed the corresponding DLCA homoaggregation measurements for both experimental systems at 1.0*M* KBr and compared the obtained CSDs with the data shown in Fig. 2(a). No significant differences were found and even the finer details of typical DLCA processes such as the fast monomer decay at large aggregation times could be observed [25].

Furthermore, we calculated the initial monomer-monomer reaction rate constant, $k_{11}$, from time evolution of the monomer concentration following the method described in Ref. [26]. This allows us to compare the aggregation velocity of the three experimental systems quantitatively and to contrast the obtained results with other DLCA data reported in the literature. For the homoaggregation experiments at 1.0*M* KBr, we obtained $(3.8\pm0.4)\times10^{-12}$ cm$^3$ s$^{-1}$ and $(4.7\pm0.5)\times10^{-12}$ cm$^3$ s$^{-1}$ for the anionic and cationic particles, respectively. For the heteroaggregation experiment at the same electrolyte concentration, $k_{11}=(4.3\pm0.4)\times10^{-12}$ cm$^3$ s$^{-1}$ was determined. The three values are well comprised within the interval of $(6\pm3)\times10^{-12}$ cm$^3$ s$^{-1}$ given by Sonntag and Strenge [27] as average value for experimental DLCA measurements. Please note that this value is substantially smaller than the theoretical von Smoluchowski limit of $k_{11}^{\mathrm{Smol}}=11.1\times10^{-12}$ cm$^3$ s$^{-1}$ for 20 °C. This discrepancy, systematically found in the literature [21,25–31], is usually explained as a consequence of the interplay between London–van der Waals forces and hydrodynamic interactions, which typically reduces the theoretically predicted rate constant by a factor of approximately 2 [28,29]. Hence, we conclude that also the 1:1 mixture aggregates in the DLCA regime at 1.0*M* although homoaggregation and heteroaggregation are taking place simultaneously. This finding indicates, furthermore, that the positively and negatively charged particles behave in a very similar way once the electrostatic interactions are completely screened.

The CSDs for the pure heteroaggregation processes arising at 10m*M* and 1.0m*M* KBr are shown in Figs. 2(b) and 2(c), respectively. Both CSDs in this low electrolyte concentration region are very similar among each other and do not differ very much from the DLCA regime occurring at high electrolyte concentration [see Fig. 2(a)]. Only at large aggregation times, some significant differences can be observed. There, the monomer concentration curves remain always above and quite separate from the other *n*-mer concentration curves. This means that the monomer behavior differs quite strongly from the one of all the other aggregates. In this sense, cluster discrimination is detected for monomers.

For short aggregation times, however, the monomer concentration curves are practically the same as in the DLCA case. Hence, also the initial monomer decay rates, which are frequently considered as a measure of the aggregation kinetics [26], are identical. This is quite surprising since homoaggregation is forbidden at electrolyte concentrations below 10m*M* and so, only one half of the total number of monomer-monomer encounters, i.e., those between unlike particles, are able to form a dimer. Thus, two oppositely charged colloidal particles aggregate roughly twice as fast as two freely diffusing particles. This means that the attractive interactions between unlike particles start to play an important role. At very low electrolyte concentrations [see Figs. 2(d) to 2(f)], the monomer aggregation rates rise even further revealing a yet increased importance of the attractive electrostatic interaction between the oppositely charged particles. For the aggregation experiment without any added electrolyte, this effect becomes so strong that the dimer maximum is reached even before the first data point in the corresponding plot.

Since the strength of the attractive electrostatic interactions increases with decreasing electrolyte concentration, it is not surprising to observe that the concentrations of all clusters decrease faster, the lower the electrolyte concentration becomes. This tendency, however, is most pronounced for dimers and grows for them up to the point at which the dimer concentration curves at very low electrolyte concentration separate completely from all the other *n*-mer concentration curves [see Fig. 2(f)]. Hence, also dimer discrimination is now observed.

Dimer discrimination is even better appreciated in Fig. 3, where the cluster concentration profiles at a fixed, relatively large time, $t_0$, are shown for different electrolyte concentrations in a semilogarithmic scale. As expected, the cluster concentration profile, $c_n(n)$, decays exponentially in the DLCA limit. This exponentially decaying behavior is maintained for clusters larger than dimers although the cluster concentrations and the slope of the curves diminish for decreasing electrolyte concentration. Only the monomers and dimers abandon this exponential behavior. As can be observed, the monomer concentration is always higher and the dimer concentration is always lower than the value that could

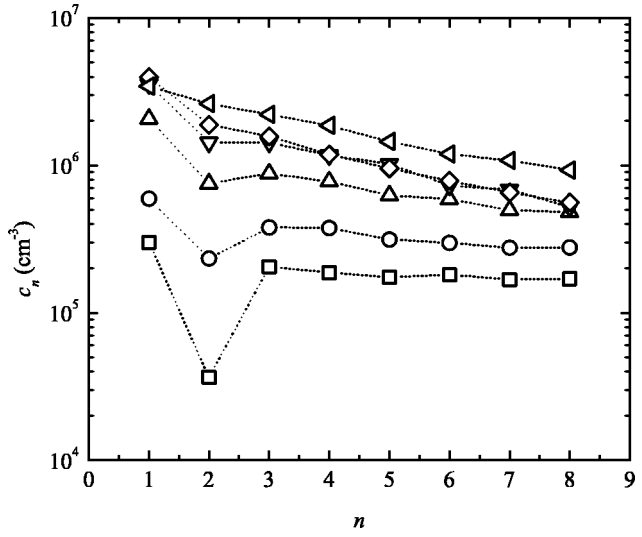


FIG. 3. Cluster concentration profiles at fixed time ($t_0 \approx 2 \times 10^4$s) for different KBr concentrations: 1.0$M$ (◁), 10m$M$ (◇), 1.0m$M$ (▽), 0.1m$M$ (△), 0.01m$M$ (○), and no added KBr (□).

be extrapolated from the exponential decay curve defined by the larger clusters. It should also be mentioned that dimer discrimination starts to become relevant at lower electrolyte concentrations than monomer discrimination. According to this tendency, trimer discrimination would be expected at an even lower ionic concentration. Under the given experimental conditions, however, this effect could not be observed since it was not possible to obtain samples with ionic concentrations below the limit given by the $p$H of the aqueous medium.

It is important to throw into relief that cluster discrimination is not just a consequence of the absence of homoaggregation. As mentioned before, the probability for the reaction between two like particles is already negligible at 10m$M$ KBr and aggregation at this electrolyte concentration is completely due to heteroaggregation. Nevertheless, only monomer discrimination is observed. As can be seen in Fig. 3, the electrolyte concentration has to drop below approximately 1m$M$ before dimer discrimination starts to become relevant. The origin of cluster discrimination seems instead to be related to the ratio between the cluster size and the range of the attractive electrostatic interactions. As the ionic concentration decreases, the thickness of the electric double layer and, consequently, the range of the corresponding electrostatic interaction increase. The relative increase of the range of the electrostatic interactions with respect to the cluster size is, however, more pronounced for smaller aggregates than for larger ones. Hence, all phenomena related to the range of the attractive electrostatic interactions are expected to be observable first for smaller aggregates and then for larger ones. This is exactly what we observed for cluster discrimination.

### B. Comparison with Brownian dynamics simulations

In the second part of this work, we now compare the experimental results with the predictions made by Puertas *et al.* [11] by means of Brownian dynamics simulations (BDS). Their simulations were performed for 1:1 mixtures of perfect microspheres of identical size and opposite surface charge. As particle-particle interactions, London–van der Waals forces and double layer overlapping in the linear superposition approximation were taken into account. Nevertheless, other important effects such as internal cluster rearrangement, aggregate rotation, hydrodynamic interactions, or aggregate sedimentation were not considered. Although typical values for the particle characteristics such as the Hamaker constant and electric surface potentials were chosen for the simulations, an exact equivalency with our experimental system is not expected.

In order to make a direct comparison between experiment and simulation possible, the particle size, the cluster concentrations, the time scale and the range of the interactions had to be normalized. For this purpose, the inverse of the Debye length, $\kappa$, was used. It is related to the concentration $c_e$ of a 1:1 electrolyte by $\varepsilon\varepsilon_0 k_B T \kappa^2 = 2e_0^2 c_e$, where $\varepsilon\varepsilon_0$ is the dielectric constant of the medium, $k_B T$ is the thermal energy, and $e_0$ is the electron charge. The Debye screening length, $\kappa^{-1}$, can be considered as an estimation of the electrical double layer thickness. Consequently, the adimensional parameter $\kappa a$ provides a suitable normalization for the particle size and the range of the electrostatic interactions. The cluster concentrations $c_n$ are easily normalized by dividing them by the initial particle concentration $c_0$. Although the particle concentration used for the simulations is about 2390 times the experimental one, it can still be considered a dilute system since only binary reactions occur. Time scale normalization, however, has to be done in such a way that equivalent aggregation stages of the experimental and simulated processes are compared. Here, we used the normalized total number of clusters as an intrinsic time scale. This quantity is not only unequivocally related to time but also has the best statistics of all the experimentally available data.

Before we compare the experimental and simulated data in a more quantitative way, we would like to make some general remarks. Just like in our experimental CSD data, monomer discrimination appears in the BDS already for $\kappa a$ values above 10 while dimer discrimination becomes observable for $\kappa a$ values below approximately 5. Discrimination of larger clusters was not found experimentally. In the simulations, cluster discrimination was detected even for aggregates as large as octamers. This octamer discrimination, however, is only observed for the smallest $\kappa a$ value used in the simulations ($\kappa a = 0.1$). Puertas *et al.* suggested that in the zero $\kappa a$ limit an odd-even cluster discrimination would be achieved with a strong bias of clusters formed by an even number of constituent particles. This hypothesis could not be confirmed experimentally since it was not possible to achieve $\kappa a$ values below 1 with our SCLS instrument because a minimal particle radius of 250 nm is required to ensure correct monomer detection [21]. Nevertheless, the experimentally observed monomer and dimer discrimination are compatible with the predicted odd-even behavior, i.e., the monomers become dominant and the dimers are biased in the CSDs.

For a more quantitative comparison between experiment and simulation, we calculated the dimer-trimer concentration ratio, $c_2/c_3$, at a fixed, relatively advanced aggregation stage

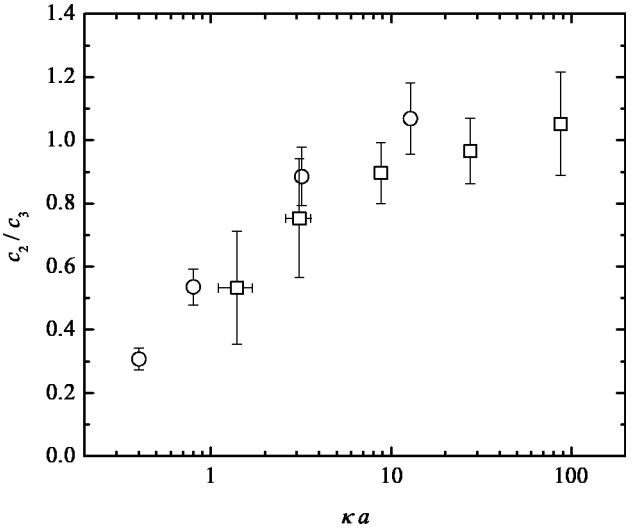


FIG. 4. Dimer-trimer concentration ratio, $c_2/c_3$, at an advanced aggregation stage as a function of $\kappa a$. The plot shows the experimental SCLS data (□) and the BDS data (○) simulated by Puertas *et al.* [11].

where the total number of clusters had dropped to one tenth of its initial value. The obtained results are plotted in Fig. 4 as a function of $\kappa a$. As can be seen in the figure, the experimental and simulated data are in good agreement in their common $\kappa a$ interval and seem to follow a single curve over the entire $\kappa a$ range. For $\kappa a$ values larger than 10, the dimer-trimer concentration ratio does not vary very much and its value remains close to unity. This means that dimers and trimers behave in similar way in the region where dimer discrimination was not observed experimentally. At lower $\kappa a$ values, however, this is not the case anymore. There, the dimer-trimer concentration ratio decreases and drops to lower values the lower the electrolyte concentration becomes. In other words, the dimers reach a more advanced state than the trimers. In this sense, dimer discrimination becomes stronger for decreasing $\kappa a$.

Finally, it should be mentioned that a similar good agreement between experiment and simulation was achieved also for other concentration ratios. Taking into account the objections made at the beginning of this section, it is quite surprising to see such a quantitative agreement.

## IV. CONCLUSIONS

Cluster discrimination was found experimentally in heteroaggregation processes arising in 1:1 mixtures of positively and negatively charged particles at low and very low ionic concentrations. Monomer discrimination could be detected already at 10m$M$ KBr while dimer discrimination started to appear only for electrolyte concentrations smaller than 1.0m$M$. This shows that cluster discrimination is not an intrinsic property of pure heteroaggregation processes since it has not fully developed as soon as homoaggregation processes are completely absent. Furthermore, dimer discrimination was observed to become more pronounced for decreasing ionic concentrations. This finding implies that cluster discrimination is most likely related to the range of the attractive electrostatic interactions between the oppositely charged particles.

The experimental results were also compared with the Brownian dynamics simulation performed by Puertas *et al.* Not only qualitative but also quantitative agreement was obtained when the adequate normalizations were performed. Especially, the onset and the increasing strength of dimer discrimination were predicted quite satisfactorily by the BDS. In their simulations, Puertas *et al.* found that cluster discrimination gives rise to an odd-even behavior in the cluster concentration profiles, i.e., odd size clusters become dominant while even size clusters are biased in the CSDs. The experimental data confirm this prediction for monomers and dimers. It should be pointed out that the simulations were performed as a function of $\kappa a$, i.e., changing only the relative range of the electrostatic interactions. Hence, the good agreement between experiment and simulations supports the above mentioned hypothesis that the cluster discrimination phenomenon originates mainly from long range electrostatic interactions.

## ACKNOWLEDGMENTS

This work was supported by the Ministerio de Ciencia y Tecnología [Plan Nacional de Investigación Científica, Desarrollo e Innovación Tecnológica (I+D+I), Project No. MAT 2003-08356-C04-01]. We thank Dr. A. M. Puertas for the helpful discussions.

[1] P. Bandini, C.A. Prestidge, and J. Ralston, Minerals Eng. **14**, 487 (2001).
[2] H. Hayashi, T. Nihei, M. Ono, S. Tsuneda, A. Hirata, and H. Sasaky, J. Colloid Interface Sci. **243**, 109 (2001).
[3] J.M. Sunkel and J.C. Berg, J. Colloid Interface Sci. **179**, 618 (1996).
[4] X. Miao and P.M. Marquis, Nanostruct. Mater. **1**, 31 (1992).
[5] B.V. Derjaguin and L. Landau, Acta Physicochim. URSS **14**, 633 (1941).
[6] E. J. W. Verwey and J. T. G. Overbeek, *Theory of the Stability of Lyophobic Colloids* (Elsevier, Amsterdam, 1948).
[7] A.M. Islam, B.Z. Chowdhry, and M.J. Snowden, Adv. Colloid Interface Sci. **62**, 109 (1995).
[8] R. Hidalgo-Álvarez, A. Martín, A. Fernández, D. Bastos, F. Martínez, and F.J. de las Nieves, Adv. Colloid Interface Sci. **67**, 1 (1996).
[9] R. Hogg, T.W. Healy, and D.W. Fuerstenau, Trans. Faraday Soc. **62**, 1638 (1966).
[10] N. Ryde and E. Matijević, J. Chem. Soc., Faraday Trans. **90**, 167 (1994).
[11] A.M. Puertas, A. Fernández-Barbero, and F.J. de las Nieves, Physica A **304**, 340 (2002).
[12] S. Stoll and E. Pefferkorn, J. Colloid Interface Sci. **160**, 149 (1993).

[13] J.A. Maroto and F.J. de las Nieves, Colloids Surf., A **132**, 153 (1998).
[14] A.M. Puertas, J.A. Maroto, A. Fernández-Barbero, and F.J. de las Nieves, Phys. Rev. E **59**, 1943 (1999).
[15] A.Y. Kim and J.C. Berg, J. Colloid Interface Sci. **229**, 607 (2000).
[16] A. Fernández-Barbero and B. Vincent, Phys. Rev. E **63**, 011509 (2001).
[17] A.M. Puertas, A. Fernández-Barbero, and F.J. de las Nieves, J. Chem. Phys. **115**, 5662 (2001).
[18] A.Y. Kim, K.D. Hauch, J.C. Berg, J.E. Martin, and R.A. Anderson, J. Colloid Interface Sci. **260**, 149 (2003).
[19] R.O. James, A. Homola, and T.W. Healy, J. Chem. Soc., Faraday Trans. **173**, 436 (1977).
[20] J.W. Goodwin, J. Hearn, C.C. Ho, and R.H. Ottewill, Colloids Polym. Sci. **252**, 464 (1974).
[21] A. Fernández-Barbero, A. Schmitt, M. Cabrerizo-Vílchez, and R. Martínez-García, Physica A **230**, 53 (1996).
[22] A. Fernández-Barbero, M. Cabrerizo-Vílchez, R. Martínez-García, and R. Hidalgo-Álvarez, Phys. Rev. E **53**, 4981 (1996).
[23] M.Y. Lin, H.M. Lindsay, D.A. Weitz, R. Klein, R.C. Ball, and P. Meakin, J. Phys.: Condens. Matter **2**, 3093 (1990).
[24] J. M. López-López, A. Schmitt, J. Callejas-Fernández, and R. Hidalgo-Álvarez, Prog. Colloid Polym. Sci. (to be published).
[25] A. Schmitt, G. Odriozola, A. Moncho-Jordá, J. Callejas-Fernández, R. Martínez-García, and R. Hidalgo-Álvarez, Phys. Rev. E **62**, 8335 (2000).
[26] H. Holthoff, A. Schmitt, A. Fernández-Barbero, M. Borkovec, M.Á. Cabrerizo-Vílchez, P. Schurtenberger, and R. Hidalgo-Álvarez, J. Colloid Interface Sci. **192**, 463 (1997).
[27] H. Sonntag and K. Strenge, *Coagulation Kinetics and Structure Formation* (Plenum Press, New York, 1987).
[28] L.A. Spielman, J. Colloid Interface Sci. **33**, 562 (1970).
[29] E.P. Honig, G.J. Roebersen, and P.H. Wiersema, J. Colloid Interface Sci. **36**, 97 (1971).
[30] M.M. Takayashu and F. Galembeck, J. Colloid Interface Sci. **155**, 16 (1993).
[31] A. Fernández-Barbero, A. Martín-Rodríguez, J. Callejas-Fernández, and R. Hidalgo-Álvarez, J. Colloid Interface Sci. **162**, 257 (1994).